J Physiol 588.21 (2010) pp 4303–4315

The Journal of Physiology

Transgene expression and effective gene silencing in vagal afferent neurons *in vivo* using recombinant adeno-associated virus vectors

M. Kollarik[1], M. J. Carr[2], F. Ru[1], C. J. A. Ring[3], V. J. Hart[3], P. Murdock[4], A. C. Myers[1], Y. Muroi[1] and B. J. Undem[1]

[1] *The Johns Hopkins School of Medicine, Baltimore, MD 21224, USA*
[2] *Discovery Biology, Respiratory Center for Excellence in Drug Discovery, GlaxoSmithKline Pharmaceuticals, King of Prussia, PA, USA*
[3] *Gene Interference and* [4] *Discovery Technology Group, GlaxoSmithKline R&D, Stevenage, UK*

Vagal afferent fibres innervating thoracic structures such as the respiratory tract and oesophagus are diverse, comprising several subtypes of functionally distinct C-fibres and A-fibres. Both morphological and functional studies of these nerve subtypes would be advanced by selective, effective and long-term transduction of vagal afferent neurons with viral vectors. Here we addressed the hypothesis that vagal sensory neurons can be transduced with adeno-associated virus (AAV) vectors *in vivo*, in a manner that would be useful for morphological assessment of nerve terminals, using enhanced green fluorescent protein (eGFP), as well as for the selective knock-down of specific genes of interest in a tissue-selective manner. We found that a direct microinjection of AAV vectors into the vagal nodose ganglia *in vivo* leads to selective, effective and long-lasting transduction of the vast majority of primary sensory vagal neurons without transduction of parasympathetic efferent neurons. The transduction of vagal neurons by pseudoserotype AAV2/8 vectors *in vivo* is sufficiently efficient such that it can be used to functionally silence TRPV1 gene expression using short hairpin RNA (shRNA). The eGFP encoded by AAV vectors is robustly transported to both the central and peripheral terminals of transduced vagal afferent neurons allowing for bright imaging of the nerve endings in living tissues and suitable for structure–function studies of vagal afferent nerve endings. Finally, the AAV2/8 vectors are efficiently taken up by the vagal nerve terminals in the visceral tissue and retrogradely transported to the cell body, allowing for tissue-specific transduction.

(Received 21 May 2010; accepted after revision 19 August 2010; first published online 24 August 2010)
Corresponding author B. J. Undem: Johns Hopkins Asthma Center, 5501 Hopkins Bayview Circle, Baltimore, MD 21224, USA. Email: bundem@jhmi.edu

Abbreviations AAV vector, adeno-associated virus vector; DRG, dorsal root ganglion; eGFP, enhanced green fluorescent protein; shRNA, short hairpin RNA.

Introduction

Visceral organs receive their sensory innervation from dorsal root ganglion (DRG) neurons, and neurons situated in vagal sensory ganglia. The vagal ganglia are referred to as the nodose ganglion and the jugular (or supranodose ganglion), with the majority of vagal neurons in the former. Nearly all vagal sensory neurons innervating subdiaphragmatic structures are unmyelinated C-fibres (Agostoni *et al.* 1957; Gabella & Pease, 1973; Asala & Bower, 1986). Vagal afferent fibres innervating thoracic structures such as the respiratory tract and oesophagus, however, are more diverse comprising about 50% unmyelinated C-fibres and 50% myelinated A fibres. Considered as a whole, the vagal afferent nervous system plays an important role in homeostasis by regulating autonomic neural tone. In addition, by evoking nocifensive responses and reflexes, vagal afferent fibres probably play an important role in tissue defense (Kollarik *et al.* 2010).

Vagal sensory A-fibres comprise primarily low-threshold stretch-sensitive receptors. These are referred to as slowly adapting and rapidly adapting receptors in the lungs (Sant'Ambrogio & Widdicombe, 2001) and as tension (mechano)receptors (structurally intraganglionic laminar nerve endings, IGLEs) in the oesophagus

DOI: 10.1113/jphysiol.2010.192971

(Zagorodnyuk & Brookes, 2000; Zagorodnyuk *et al.* 2003). In addition, a touch- and acid-sensitive Aδ 'cough receptor' has been described in the trachea (Canning *et al.* 2004; Mazzone *et al.* 2009). With respect to C-fibres, two distinct phenotypes of capsaicin-sensitive nociceptive C-fibres, referred to as neural crest C-fibres and placodal C-fibres, have been identified in both the respiratory tract and oesophagus (Undem *et al.* 2004; Kollarik *et al.* 2010). There may be additional vagal afferent phenotypes that terminate in specialized neuroepithelial bodies in the airways (Adriaensen *et al.* 2006). These vagal afferent nerve subtypes innervating thoracic structures have different activation profiles: they terminate in different tissue regions, express different neuromodulatory ion channels, and result in different reflexes and sensations upon activation. Our knowledge about the physiology of these nerves has been gained mainly from studies using extracellular electrophysiological recordings, and morphological analysis using standard immunohistochemical techniques or histological examination of tissues following injection of neuronal tracing dyes. Studies on the role of specific ion channels have been limited, and for the most part dependent on pharmacological analyses.

Both the morphological and functional studies of the complex vagal sensory innervation would be aided by a mechanism that would allow selective transduction of neurons with specific viral vector-selected genes and molecular tools. In the past decade strides have been made in the use of viral vectors in the study of the nervous system. Much of this work has focused on the central nervous system. In the peripheral nervous system, studies of viral gene transfer have focused mainly on the DRG neurons, and studies relating to pain (Glatzel *et al.* 2000; Xu *et al.* 2003*b*; Storek *et al.* 2008; Mason *et al.* 2010). There are few, if any, studies that report the use of recombinant viral technology in the study of the structure or function of vagal afferent neurons.

Adeno-associated viruses have proven useful in the transduction of post-mitotic non-dividing neurons. This viral vector is safe, non-replicating and has the advantage of resulting in long-lived transduction (Xu *et al.* 2003*b*). Although *in vitro* studies using neurons isolated and cultured from nodose ganglia have shown the feasibility of this approach, there is little information regarding AAV-associated transduction of vagal sensory neurons *in vivo*. In the present study we addressed the hypothesis that vagal sensory neurons can be transduced with AAV vectors *in vivo*, in a manner that would be useful for morphological assessment of nerve terminals, using enhanced green fluorescent protein (eGFP), as well as for the selective knock-down of specific genes of interest in a tissue-selective manner.

Methods

In vivo transfection of vagal primary afferent neurons

All experiments were approved by the Johns Hopkins Animal Care and Use Committee. Male Hartley guinea pigs (Hilltop Lab Animals, Inc., Scottsdale, PA, USA), weighing 100–200 g at the beginning of the experiment, were used. The guinea pigs were briefly anaesthetized with ketamine (50 mg kg^{-1}) and xylazine (10 mg kg^{-1}). Lateral neck skin incision (10–15 mm long) was made over superficial masseter muscle. The vagal nodose ganglion with adjacent vagus nerve was exposed by careful blunt preparation. An aluminum-silicate pipette was filled through the tip (tip diameter 50–100 μm) by capillary effect with 2–3 μl of solution containing the virus vector. The pipette was connected via polyethylene tube to the manually controlled pressure source (calculated pressure 5–10 kPa) and injected into the nodose ganglion under visual control (10×, dissection scope). The pressure was adjusted based on visual evaluation of the injection rate so as the volume of the vector was injected into the ganglion over 1–2 min. Appropriate sterile and safety (biosafety 2) procedures were followed. AAV2 (adeno-associated virus 2)-based vectors pseudotyped with AAV2, AAV7, AAV8 and AAV9 serotype capsids (Gao *et al.* 2002) (AAV2/2, AAV2/7, AAV2/8 and AAV2/9) were obtained from Penn Vector Core, Gene Therapy Program, University of Pennsylvania supplied in titres 1–3 × 10^{12} PFU.

Histology and immunohistochemistry

The animals were killed by a CO_2 overdose and exsanguination. Intrathoracic organs and sensory vagal ganglia (jugular and nodose ganglia) were isolated and fixed in 4% formaldehyde at 4°C overnight and for 2 h, respectively. The tissues were rinsed in PBS and cryoprotected in sucrose (18%, overnight). Continuous serial cryostat sections (12 μm thick) of the entire vagal ganglion (nodose or jugular) were thaw-mounted on four different slides, such that the first slide had sections 1, 5, 9 . . . , the second 2, 6, 10 . . . and so on; alternate slides were used for the analysis. Slides were mounted and rinsed with water and PBS (2×). For quantification of eGFP in sections of vagal ganglia, the slides were coverslipped in PBS and viewed immediately. For immunohistochemistry, the slides were incubated with goat serum (10% in PBS) containing Tween 20 (0.5%) and bovine serum albumin (BSA, 1%) at room temperature for 1 h. Sections were then covered with primary antibodies diluted in PBS containing Triton X-100 (0.3%) and BSA (1%) (Triton/BSA–PBS) for 24 h at 4°C. After rinsing (3×) with Triton–BSA–PBS the sections were covered with secondary (anti-primary) antibodies diluted in Triton–BSA–PBS for 2 h at room

temperature. The sections were then rinsed with PBS (2×), and saline buffered with phosphate to pH 8.6, and coverslipped with anti-fade glycerol (antifade kit Fluoro-mount, Invitrogen, Carlsbad, CA, USA). Staining for neurofilament 160 kD (NF) was performed using mouse anti-NF (1:400, Chemicon, Temecula, CA, USA) as primary antibody, and goat anti-mouse Alexa Fluor 594-labelled secondary antibody (1:100, Invitrogen). Sections were examined under epifluorescence (Olympus DX60) using appropriate filter combinations for eGFP (excitation filter 450–480 nm, barrier filter 500–515 nm) and for Alexa Fluor 594 (excitation filter 510–550 nm, barrier filter 570–590 nm). Trachea, bronchi and lung parenchyma as well as heart, oesophagus and adjacent connective tissue were cut in 1–2 mm sections and evaluated for the presence and localization of the neuronal tracer. For whole-mount preparation of fresh (living) tissue, the trachea and oesophagus were dissected, cut longitudinally and pinned flat in a Sylgard dish filled with PBS. The tracheal epithelium was removed by gentle brush and the oesophageal mucosal layer was dissected in some preparations from the trachea and oesophagus, respectively. For confocal imaging the trachea and oesophagus were fixed as described above, rinsed with PBS and pressure coverslipped with anti-fade glycerol (pH 6.8). For whole-mount staining the tracheal and oesophageal tissue preparations were fixed as described above, washed in PBS (3 × 20 min), incubated with goat serum (10% in PBS) containing Tween 20 (2.5%) and bovine serum albumin (BSA, 1%) at 4°C for 4–9 h, washed with PBS (3 × 20 min), incubated with rabbit anti-GFP primary antibody (Molecular Probes, A-11122) diluted 1:500 in Triton–BSA–PBS for 48 h at 4°C, washed with Triton–BSA–PBS (3 × 20 min, room temperature), incubated with goat anti-rabbit Alexa Fluor 488 secondary antibody (Invitrogen, A11008) diluted 1:100 in Triton–BSA–PBS for 4 h at room temperature, washed in PBS (3 × 30 min), incubated in anti-fade glycerol (pH 6.8) for 24 h at 4°C and pressure coverslipped with anti-fade glycerol. The brainstem was fixed for 12–24 h in 4% formaldehyde and cryoprotected in sucrose (18%). Transversal cryostatic brainstem 50 μm sections −2 mm to 3 mm from obex were evaluated.

Generation of AAV8-based, guinea pig TRPV1-targeting shRNA vectors

Four shRNA sequences were designed to target the expression of guinea pig TRPV1 using a commercial siRNA design program (Dharmacon Inc., Boulder, CO, USA). Oligonucleotides were synthesized (Invitrogen, Paisley, UK), annealed and cloned downstream of the human U6 promoter in a derivative of the pENTR1A plasmid (Invitrogen) generated at GlaxoSmithKline. A negative control shRNA, based upon sequence of a commercially available negative control siRNA (Dharmacon Inc.) was also generated. The TRPV1-targeting shRNA plasmids were evaluated for their efficiency in suppressing the expression of guinea pig TRPV1 by co-transfection into the guinea pig fibroblast cell line 104c1 (Evans *et al.* 1975) with a guinea pig TRPV1-expression plasmid (pCIN5-gpTRPV1, generated at GlaxoSmithKline) using an in-house surfactant GSK347232 (Castro *et al.* 2004). Efficiency of gene suppression was determined by TaqMan analysis using the primer and probe sequences for guinea pig TRPV1 (Table 1). One of the shRNA clones exhibiting the highest degree of TPRV1 knockdown was selected for further study. The gpTRPV1-targeting shRNAs is as follows: 5′-GATATCCTTCTGCTCAATATTTCAAGAGA ATATTGAGCAGAAGGATAT-3′. The sequence of the negative control shRNA is as follows: 5′-GTAGCGAC-TAAACACATCAATTCAAGAGATTGATGTGTTTAGTC-GCTA-3′. Underlining denotes the sense and antisense sequences of the shRNA separated by a 'loop' sequence. The U6 promoter – shRNA-expression cassettes from this shRNA plasmid – were subcloned into the AAV2-based shuttle plasmid pZAC2.1eGFP3 (kind gift of Dr Jim Wilson, Gene Therapy Program, University of Pennsylvania) and AAV8-based vectors were generated by the triple plasmid co-transfection method (Gao *et al.* 2002) and titrated by TaqMan analysis at the Vector Core, Gene Therapy Program, University of Pennsylvania).

Cell dissociation and picking

After the animals were killed by 100% CO_2 asphyxiation, the vagal ganglia were rapidly dissected and cleared of adhering connective tissue. The isolated tissue was incubated in the enzyme buffer (2 mg ml^{-1} of collagenase type 1A and 2 mg ml^{-1} of dispase II in 2 ml of Ca^{2+}-, Mg^{2+}-free Hanks' balanced salt solution) for 50 min at 37°C. Neurons were dissociated by trituration with three fire-polished glass Pasteur pipettes of decreasing tip pore size, then washed by centrifugation (3 times at 700 *g* for 3 min) in L-15 medium containing 10% fetal bovine serum (FBS). The cells were then resuspended in 100–150 μl of L-15 medium containing 10% FBS. The cell suspension was transferred onto circular 25 mm glass coverslips (Bellco Glass Inc., Vineland, NJ, USA) coated with poly-D-lysine (0.1 mg ml^{-1}), 25 μl per coverslip. After the suspended neurons had adhered to the coverslips for 2 h, the neuron-attached coverslips were flooded with L-15 medium containing 10% FBS and used within 24 h. The coverslips were used for intracellular calcium imaging and patch clamp studies as described below. For cell collection the coverslips were continuously perfused with PBS and the eGFP-expressing cells identified by green fluorescence were collected into the borosilicate pipette pulled to tip

Table 1. Sequences of primers and probes used for qRT-PCR analysis

Gene	Primer (forward/reverse) sequence (5′–3′)	Probe sequence (5′–3′)	Sequence ID
TRPV1	CCTGGGAGCCAAACTCTACCC TGGTTCCGGGATCTCTCTCTG	TTCACACCACTGGCTCTGGCTGCTAGC	NM_001172652.1
Nav1.3 α subunit	AGCTTCCAGGGTGGATTGC CTGCTTGCTCCCATTCTCAAC	TGCACCACCAGACTGCGACCCT	VAAKN01597291
Nav1.7 α subunit	TTTTGCGGCTGCCCTAGA CATGGCAATGAGCTGGACTTT	CCCCCTCTTCTCATAGCAAAACCTAA	AAKN01307579
Nav1.8 α subunit	CTCTTCCGAGTCATCCGCCT GCCCGATGTTGAAGAGAGCA	CACGCTGCTCTTTGCCCTCATGATGTC	CQ891331
ASIC3	GGAGCGGGTGCAGTACTATGG TGATGTTGCACAGGGTGACG	CACGAAACAGTCCTGGACGAGCGTGAG	scaffold_32:773504-776659*
GAPDH	CAAGGTCATCCATGACAACTTTG GGGCCATCCACAGTCTTCTG	ACCACAGTCCATGCCATCACTGCCA	EU862201

*Deduced from *Cavia porcellus* draft assembly (Broad Institute cavPor3, Feb. 2008), UCSC Genome Bioinformatics Group.

diameter 50–100 μm by using negative pressure. Twenty to forty neurons were collected per individual sample. For negative control experiments a sample of superfusing PBS was collected.

Quantitative RT-PCR analysis

Samples containing pooled neurons (approx. 5–10 μl) were mixed with 20 μl 1× Turbo-Capture 384 RNA kit lysis buffer (Qiagen, CA, USA) and pooled again as necessary to gain ∼50 neurons per pooled sample. Lysed neuron samples were added to a Turbo-Capture 384 kit RNA-binding plate, with removal of unbound material and repeat addition/binding of the excess sample as required, followed by RNA purification according to the manufacturer's instructions (Qiagen). RNA was then stored at −80°C until use. The pooled RNA samples were reverse transcribed in duplicate (RT+) using random priming, with a negative control omitting the reverse transcriptase (RT–), according to manufacturer's instructions (25°C for 10 min, 37°C for 2 h, and 70°C for 5 min; cDNA archive kit and ABI9700 instrument, Applied Biosystems, Foster City). Pre-amplification of samples and their replicates (RT+ and RT−) was performed using a multiplex mix of all primers (final primer concentration 400 nM, Table 1) using TaqMan Universal PCR Mastermix containing uracil-*N*-glycosylase (UNG) (50°C for 2 min, 95°C for 10 min, 10 cycles of 95°C for 15 s and 60°C for 1 min, ABI9700 instrument; Applied Biosystems). The 20 μl of each pre-amplification product was then diluted by adding 30 μl water and mixing, followed by the transfer of a 2 μl volume of each sample to multiple 384-well optical PCR plates. Single gene measurement was accomplished by the addition of 8 μl TaqMan Universal PCR Master Mix (Applied Biosystems), excluding UNG, and containing the appropriate single gene primers (final concentration 900 nM each) and probe (final concentration 100 nM), to each well of a single plate using Biomek FX robotics (Beckman-Coulter). Plates were cycled on an AB7900HT TaqMan instrument (95°C for 10 min, 40 cycles of 95°C for 15 s and 60°C for 1 min). Data were collected and analysed using SDS v.2.2.2 and exported into Excel where duplicate measurements of each RNA sample were checked for good concordance and then averaged, while RT– measurements were checked for negligible signal. Gene mRNA abundance in each sample was calculated using a standard curve of sheared genomic DNA and normalized to GAPDH abundance in the respective sample. The expression of evaluated ion channels was compared by using one-way ANOVA. The primers for the guinea pig $Na_V1.3$, $Na_V1.7$, $Na_V1.8$ α subunits were used in the previous study (Kwong *et al.* 2008).

Patch clamp electrophysiology

Whole cell gramicidin-perforated patch clamp recordings were made from vagal jugular neurons as described previously (Yu *et al.* 2008). Briefly, the recordings were performed using Multiclamp 700A amplifier and Axograph 4.9 software. The pipette (1.5–3 MΩ) was filled with a pipette solution composed of KCl (140 mM), $CaCl_2$ (1 mM), $MgCl_2$ (2 mM), EGTA (11 mM), Hepes (10 mM) and dextrose (10 mM) titrated to pH 7.3 with KOH (304 mosmol l^{-1}) containing 2–3.5 μg ml^{-1} gramicidin. Gramicidin was dissolved in 1 mg ml^{-1} DMSO and mixed with the pipette solution just prior to each recording. After forming a gigaohm seal, cell membrane potential was held at −60 mV. In current clamp mode the pipette capacitance was neutralized by 90% of measured value. The inclusion criteria were the access resistance <30 MΩ and the membrane resistance (determined from a series of negative current steps)

>100 MΩ. In voltage clamp mode recordings were made after whole cell capacitance compensation. During the experiments, the cells were continuously superfused (6 ml min^{-1}) with Locke solution (35°C); composed of (mM): 136 NaCl, 5.6 KCl, 1.2 $MgCl_2$, 2.2 $CaCl_2$, 1.2 NaH_2PO_4, 14.3 $NaHCO_3$ and 10 dextrose, gassed with 95% O_2–5% CO_2 (pH 7.3–7.4). Capsaicin (1 μM) was delivered in superfusing solution for 1 min. The data are presented as mean ± S.E.M. of inward current density (inward current normalized for the cell capacitance, pA pF^{-1}) and compared using unpaired *t* tests. Standard whole cell ruptured patch clamp recordings were made in experiments designed to evaluate basic properties of AAV2/8 encoding control shRNA-transfected neurons. For these studies, the pipette (1.5–3 MΩ) was filled with a pipette solution composed of KCl (140 mM), $CaCl_2$ (1 mM), $MgCl_2$ (2 mM), EGTA (11 mM), Hepes (5 mM) and dextrose (10 mM) titrated to pH 7.3 with KOH (304 mosmol l^{-1}). The cells were continuously superfused with solution; composed of (mM): 140 NaCl, 3.0 KCl, 2.0 $MgCl_2$, 2.0 $CaCl_2$, 10.0 Hepes and 10 dextrose, titrated to pH 7.3 with NaOH (Cummins *et al.* 2009). Input resistance was measured by taking the slope from a straight-line fit to the voltage–current plots of five hypolarizing current steps. Action potential was obtained by injecting a series of depolarizing currents from 0 to 100 pA in 10 pA increments. A 10 to ∼40 pA injection was effective to trigger action potential in all neurons. Action potential threshold was measured at the beginning of the sharp upward rise of action potential traces. The data are presented as mean ± S.E.M. and compared using unpaired *t* tests.

Intracellular calcium measurement

The intracellular calcium measurements were done with dissociated vagal nodose neurons as described previously (Taylor-Clark *et al.* 2005). The coverslip was loaded with fura-2 AM (8 μM) in L-15 media containing 20% FBS and incubated for 40 min at 37°C. The coverslip was placed in a custom-built chamber (bath volume of 600 μl) that was superfused with Locke solution (at 35°C) for 15 min before the experiment by an infusion pump (4 ml min^{-1}). Changes in intracellular $[Ca^{2+}]_{free}$ were measured by digital microscopy (Universal, Carl Zeiss, Inc., Thornwood, NY, USA) equipped with in-house equipment for ratiometric recording of single cells. For each experiment a brightfield image and a fluorescent image was taken of cells under study. eGFP-labelled cells were clearly identifiable. The field of cells was monitored by sequential dual excitation, 352 and 380 nm, and the analysis of the image ratios used methods previously described to calculate changes in intracellular $[Ca^{2+}]_{free}$ (MacGlashan, 1989). The ratio images were acquired every 6 s. Superfused buffer was stopped 30 s prior to each drug application, when 300 μl of buffer was then removed from the bath using a taper. The drug (300 μl) was then added gently to the bath during the time period between two ratio image acquisitions. In each experiment the cells on the coverslip were first superfused with Locke solution for 240 s, then exposed to capsaicin (0.1 μM, 60 s), washed (Locke solution, 180 s), exposed to bradykinin (1 μM, 60 s), washed (180 s), exposed to KCl (75 mM, 30 s), washed (60 s) and exposed to ionomycin (0.5 μM). The response to an agonist (capsaicin or bradykinin) was considered positive if the average increase in apparent intracellular calcium concentration during 60 s following the agonist administration was more then 2 standard deviations over the average baseline during the preceding 90 s. The KCl and the ionomycin were used as control stimuli. The data are expressed relative to peak ionomycin response (%, mean ± S.E.M.). Unpaired *t* tests and ANOVA were used for statistical analysis when appropriate, and a *P* value less than 0.05 was taken as a significant difference.

Results

In vivo transfection

Four AAV pseudoserotypes, AAV2/2, 2/7, 2/8 and 2/9, each encoding the eGFP gene, were evaluated for the ability to transduce nodose neurons when injected directly into the nodose ganglion *in vivo* as described in Methods ($n = 4$ nodose ganglia for each pseudoserotype). In preliminary experiments we found only limited transduction 2 weeks following the vector injection (data not shown). By 4 to 5 weeks following the injection, however, each of the four pseudoserotypes was found effective in leading to strong eGFP production in the majority of nodose ganglion neurons as detected by green fluorescent signal in the histological sections of the nodose ganglia. The transfected ganglia revealed no gross anatomical abnormalities. Although we found that each serotype was effective in transducing vagal sensory neurons, we focused our more quantitative efforts on AAV2/8 and AAV2/2.

Figure 1*A* and *B* shows expression of eGFP in the nodose ganglia after injection of AAV2/8 and AAV2/2. We injected the nodose ganglia in three animals with AAV2/8 (3 μl, $\sim 10^{12}$ PFU ml^{-1}) and in all three ganglia we noted that 50–60% of the neurons strongly expressed eGFP (Fig. 1*B*). The number of transduced neurons per section averaged 55 ± 9 (only the neuronal profiles with clearly identifiable nuclei were counted, $n = 24$ sections from the central parts of 3 nodose ganglia). Likewise, when AAV2/2 was injected into the nodose ganglia ($n = 5$), the majority of neurons were efficiently transduced (Fig. 1*A*). The green fluorescent signal was only found in neuronal and axonal

profiles (Fig. 1*A*–*C*). In subsequent experiments, when an AAV2/8 titre was increased to $\sim 10^{13}$ PFU ml^{-1} we noted that 86 ± 4% of the nodose neurons strongly expressed eGFP 5 weeks after nodose injection ($n = 6$ nodose ganglia). The latest time point evaluated was 5 months after the injection of AAV2/8 ($\sim 10^{13}$ PFU ml^{-1}). After 5 months we found green fluorescence in approximately 70% (247/341) of neuronal profiles counted in five sections (2 randomly selected visual fields) from different parts of the ganglion.

Vagal sensory neurons comprise large neurofilament-immunoreactive neurons that project myelinated A fibres to visceral tissues, as well as small-diameter neurofilament-negative neurons that project unmyelenated C-fibres to the tissues. Both AAV2/8 (Fig. 1*C* and *D*) and AAV2/2 transduced both types of neurons in the nodose ganglion. Strongly eGFP-positive profiles were evaluated for NF160 immunoreacitivity in four to six sections of transfected ganglia. In the sections from the nodose ganglion injected with AAV2/2, a total of 152 eGFP-positive profiles were evaluated of which 75 were clearly NF-positive (49%). In sections from the nodose ganglion injected with AAV2/8, a total of 307 profiles were evaluated of which 82 were clearly NF-positive (27%). These data demonstrate that both AAV2/2 and AAV2/8 transfect NF-positive along with the NF-negative neurons. That these AAV pseudoserotypes transduce A-fibre and C-fibre neurons is further supported by the observation that the eGFP-positive structures consistent with A- and putative C-fibre peripheral terminations were found in peripheral tissues (see below).

We next evaluated the extent to which the virus transduction was delimited to the injected ganglion. This is an important issue, because thoracic organs receive vagal sensory innervation from both the nodose ganglion and jugular (supranodose ganglion). Depending on the hypothesis being addressed it may be advantageous for neurons in one ganglion to be transduced, or for vagal sensory neurons in both ganglia to be transduced. When AAV2/8 was injected into the nodose ganglion ($n = 5$), we noted that jugular ganglion neurons were also transduced, albeit with less efficiency (30–50% of jugular neurons, Fig. 1*F*). By contrast, in five experiments, when AAV2/2 was injected into the nodose ganglion, it remained delimited to the ganglion, such that virtually no neurons in the jugular ganglion were transduced (Fig. 1*E*) although effective transduction was detected in the nodose ganglia (Fig. 1*A*).

Tissue-selective transduction

We addressed the hypothesis that selective gene transfer can be obtained in a tissue-selective manner by introducing the AAV specifically to the nerve terminals within visceral tissue. We hypothesized that the viral genetic material will be transported from the peripheral terminals back to the nucleus in the distant vagal ganglia. For these experiments we chose to evaluate tissue-selective transduction in the oesophagus. We injected a total of 20 μl of AAV2/8 vector (10^{12} PFU ml^{-1}), directly into the cervical oesophageal wall in a manner identical to the injection of the retrograde tracer DiI in our previous studies (Yu *et al.* 2008). The right and left vagal sensory ganglia were harvested 7 weeks later. We found that indeed this resulted in an effective transduction of

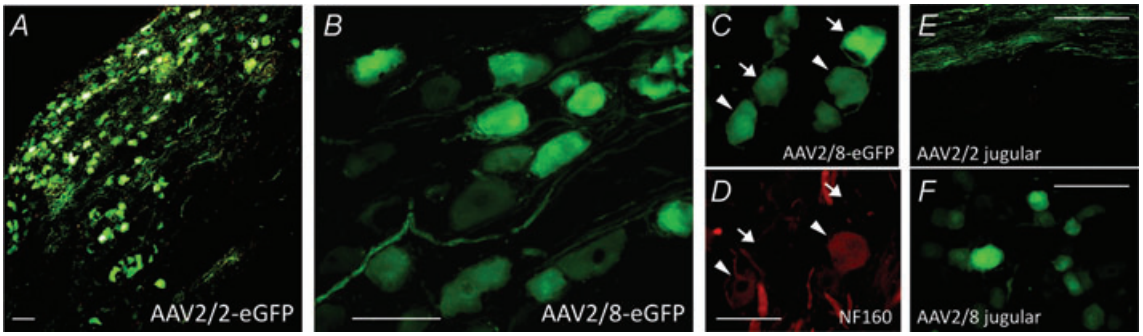

Figure 1. Effective *in vivo* transduction of vagal afferent neurons by adeno-associated virus (AAV) vectors
Enhanced green fluorescent protein (eGFP) expression detected as green fluorescence in histological sections of nodose ganglia harvested 4–5 weeks following *in vivo* injection of AAV2/2 and AAV2/8 vectors encoding eGFP into the nodose ganglia (in *A* and *B*, note the difference in scale). AAV vectors transducted both A-fibre (neurofilament NF160-positive, arrowheads) and C-fibre (neurofilament NF160-negative) nodose neurons (*C* and *D*). Injection of AAV2/8, but not AAV2/2, into the nodose ganglion resulted in effective transduction of neurons in ipsilateral jugular ganglion (*E* and *F*). Jugular ganglion shown in *E* is from the same vagus nerve as the nodose ganglion in *A*. Note eGFP-positive through fibres (central projections of the nodose neurons). Horizontal bars, 50 μm.

oesophagus-specific neurons. Figure 2 shows an example of a transduced vagal neuron. The efficacy of transduction was evaluated in dissociated jugular neurons where 10–15 transfected neurons per coverslip were identified by green fluorescencent signal ($n = 16$ coverslips from 4 guinea pigs). Identical injection of retrograde tracer DiI in our previous experiments (Yu *et al.* 2008) results in similar numbers of DiI-labelled neurons. The results are consistent with the conclusion that localized viral injection results in relatively efficient transduction of the vagal neurons innervating the site of injection.

Use of AAV to knock-down selected genes

The data show that transfection of vagal sensory neurons can lead to long-lasting transduction (and eGFP production) by recombinant AAV. It is not clear, however, whether the transduction is efficient enough to allow for an effective gene silencing strategy in the vagal sensory neurons. We addressed the question using AAV vectors encoding shRNA. To this end, we chose to evaluate the knock-down of TRPV1 expression and function in transduced vagal neurons (see Methods for details on generation of AAV2/8 vectors encoding shRNA and eGFP). The AAV2/8 vector with TRPV1-targeting shRNA, or one with a negative control shRNA, were injected into the nodose ganglia (AAV2/8 vector encoding TRPV1-targeting shRNA and control shRNA, $n = 12$ and 12 ganglia, respectively). Five weeks later we found that the expression of TRPV1 mRNA in nodose neurons transduced with AAV2/8 encoding TRPV1-targeting shRNA was reduced by >95% compared to neurons transduced with AAV2/8 encoding control shRNA as assessed by quantitative RT-PCR (Fig. 3). To evaluate whether the TRPV1-targeting shRNA causes general suppression of gene expression in nodose neurons we also analysed the expression of several other channels important for sensory function in guinea pig nodose neurons for which validated assays were available to us at the time of study (voltage-gated sodium channels Nav1.3, Nav1.7 and Nav1.8, and the acid-sensing ion channel ASIC3). Figure 3 shows that the expression of these genes was not altered. Consistent with a recent report in DRG ganglia, we noted no reduction in the numbers of nodose neurons transduced with shRNA-containing viruses (Ehlert *et al.* 2010).

By using a conventional fura-2-based calcium assay, we also found that the functional response to capsaicin in nodose neurons was greatly reduced (>85% reduction) in neurons transduced with AAV2/8 encoding TRPV1-targeting shRNA. The capsaicin response in neurons transduced with AAV2/8 encoding negative control shRNA was normal. In the whole population of the transduced neurons, the average response to capsaicin (0.1 μM, 60 s) was 12.4 ± 2.0% and 1.8 ± 0.02% of the peak ionomycin (1 μM)-induced calcium increase in neurons transduced with control shRNA ($n = 139$) and TRPV1-targeting shRNA ($n = 290$), respectively ($P < 0.01$, unpaired t test) (data in Fig. 4). The percentage of the neurons responsive to capsaicin was also greatly reduced in neurons transfected with TRPV1-targeting shRNA *vs.* control shRNA (46% *vs.* 9%, respectively, $P < 0.01$). To ascertain the integrity of our calcium assay, the neurons were also stimulated by KCl. The magnitude of the response to KCl tested when the calcium

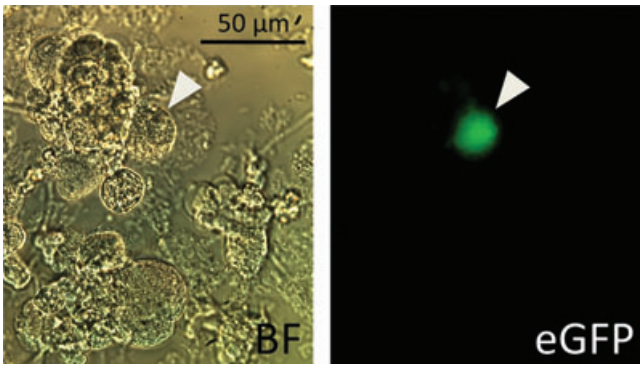

Figure 2. Transduction of vagal neurons following the injection of AAV vector into the peripheral tissue
AAV2/8 vector was injected *in vivo* into the wall of cervical oesophagus and vagal sensory ganglia were harvested 7 weeks later. BF, brightfield view of dissociated vagal nodose neurons; eGFP, fluorescent visualization of eGFP in the same field.

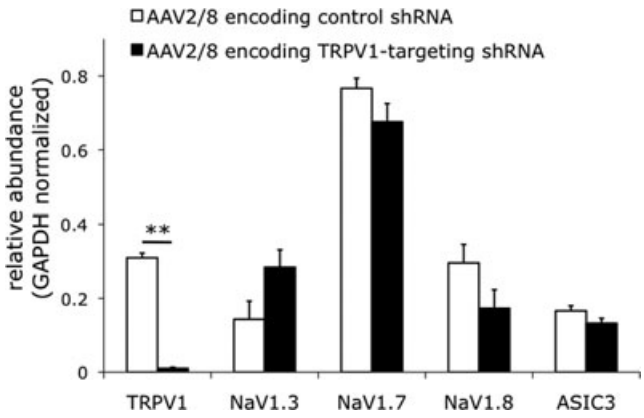

Figure 3. Knockdown of TRPV1 expression in vagal nodose neurons after *in vivo* transduction with AAV2/8 encoding TRPV1-targeting shRNA
qRT-PCR studies. For qRT-PCR studies the transducted neurons were individually collected and pooled for qRT-PCR analysis. Control shRNA, $n = 4$ (duplicates from 2 pooled samples containing a total of 106 transducted nodose neurons); TRPV1-targeting shRNA, $n = 8$ (duplicates from 4 samples containing a total of 343 transducted nodose neurons). $^{**}P < 0.01$, 1-way ANOVA followed by Bonferroni's multiple comparison test. The nodose ganglia were injected *in vivo* with the vectors encoding indicated shRNAs, harvested 4–5 weeks later, dissociated and the transducted neurons were identified by green fluorescence.

Table 2. Resting membrane potential (RMP) and action potential threshold of nodose neurons transduced with AAV2/8 vector encoding control shRNA

	n	RMP (mV)	Threshold (mV)
Naïve	7	50.7 ± 3.07	−43.0 ± 1.31
AAV2/8 control shRNA	8	50.0 ± 1.57	−46.1 ± 0.75

Data represent the mean ± S.E.M.

returned to baseline was comparable between control and TRPV1-targeting shRNA (Fig. 4).

The effect of bradykinin was not appreciably affected by the TRPV1-targeting shRNA. The magnitude of the response to bradykinin appears similar for both control and TRPV1-targeting shRNAs (Fig. 4). This conclusion, however, requires some qualification. Due to time constrains of the assay the capsaicin response did not return to the baseline before the bradykinin was added, and in many neurons this probably masked the subsequent bradykinin response. This also probably led to a low apparent percentage (14%) of bradykinin-responsive neurons in the control shRNA-treated ganglia. Nevertheless, based on previous work in our laboratory using the same assay, we know that bradykinin selectively activates approximately 60% of capsaicin-sensitive guinea pig vagal neurons (Lee *et al.* 2005). Thus, using the proportion of capsaicin-sensitive neurons in control shRNA (46%, see above), the estimated percentage of bradykinin-responsive neurons in this population is 25–35%. In agreement with this prediction, we found that approximately 30% (91/290) of neurons transduced with TRPV1-targeting shRNA were responsive to bradykinin (1 μM).

We also evaluated the ability of the AAV vector-delivered shRNA to functionally inhibit the electrophysiological response to capsaicin. We first evaluated the effect of transduction with the AAV2/8 vector encoding control shRNA on the basic electrophysiological properties of vagal neurons by the whole cell ruptured patch clamp technique. The resting membrane potential and the action potential threshold were similar between naïve neurons and the neurons transduced with AAV2/8 vector encoding control shRNA (Table 2). Input resistance evaluated in four naïve and four of these transduced neurons was also similar (719 ± 168 MΩ and 632 ± 185 MΩ, respectively). The efficacy of TRPV1 knock-down was then studied in vagal jugular sensory neurons by the whole cell gramicidin-perforated patch clamp technique. Jugular neurons that expressed eGFP were harvested 5–6 weeks following the injection of AAV2/8 encoding shRNAs into the nodose ganglia (as described above, the nodose injection of AAV2/8 effectively transduces a proportion of jugular neurons). Twelve jugular neurons from three animals transduced with control shRNA and 16 jugular neurons from four animals transduced with TRPV1-targeting shRNA were studied. Capsaicin (1 μM, 30 s) evoked robust current (peak current density >10 pA pF^{-1}) in 10 of 12 control shRNA-transduced jugular neurons (Fig. 5*A*). This is consistent with the previous observations that the majority of guinea pig jugular neurons are capsaicin sensitive (Undem *et al.* 2004; Yu *et al.* 2008). In contrast, capsaicin evoked robust current only in 2 of 16 TRPV1-targeting shRNA-transduced neurons ($P < 0.01$, χ^2 test). Notably, in 11 of 16 neurons transduced with TRPV1-targeting shRNA no measurable current was detected in response to capsaicin (Fig. 5*B*). Overall the average response to capsaicin was reduced by >85% (Fig. 5*C*). As a control stimulus, the current injection (1 nA, 2 ms) was effective to evoke action potential in all neurons.

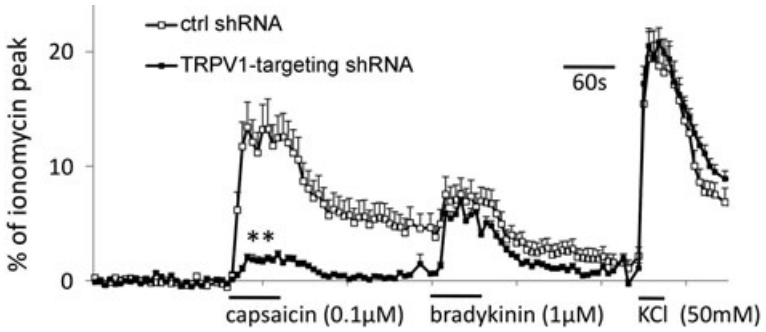

Figure 4. Knock-down of TRPV1 function in vagal nodose neurons after *in vivo* transduction with AAV2/8 encoding TRPV1-targeting shRNA

Intracellular calcium imaging studies. Response was normalized to peak intracellular calcium increase induced by ionomycin (1 μM). Control shRNA *vs.* TRPV1-targeting shRNA, $P < 0.01$ (unpaired *t* test). Control shRNA, $n = 139$ neurons in random samples from $N = 6$ transduced nodose ganglia); TRPV1-targeting shRNA, $n = 290$ nodose neurons from $N = 6$ transducted ganglia). The nodose ganglia were injected *in vivo* with the vectors encoding indicated shRNAs, harvested 4–5 weeks later, dissociated and the transducted neurons were identified by green fluorescence.

Use of AAV in morphological characterization of afferent nerve terminals

We found that the eGFP produced by vagal neurons transduced by the recombinant AAV vectors is transported to both the central and peripheral terminals of the vagal afferent neurons. With this technique we found that individual afferent nerve fibres can be followed to their termination sites in the tracheal and oesophageal wall, as well as to their central terminations in the brainstem.

The afferent nerve terminals were readily visualized in living tissues without histological processing. Figure 6*A* shows well-defined terminations of a nodose Aδ-fibre in the trachea (the tracheal epithelium was removed by gentle brush to improve visibility). When fresh tracheal preparations ($n = 5$) were perfused for 4–5 h with Krebs solution (35°C) and the labelled nerve terminals were frequently viewed (i.e. exposed to fluorescent light, total time of direct exposure >30 min), the fluorescent signal was stable for the whole period without notable reduction in intensity. Previous studies have shown that these nodose tracheal Aδ-fibres are responsible for mechanically evoked cough (Canning *et al.* 2004; Mazzone *et al.* 2009). The nodose tracheal Aδ-fibres seldom had a single termination structure. The vast majority (12/14) of nodose tracheal Aδ-fibres had two to six terminal structures all of which were situated beneath the basement membrane. Physically removing the epithelium did not disrupt the structure. The intense green fluorescent signal persisted also during the histological processing. Figure 6*B* and *C* show confocal images of the nodose Aδ-fibre terminal structure in the trachea (Fig. 6*B*), and a single intraganlionic laminar ending in the oesophagus (Fig. 6*C*) in fixed tissues.

A second clearly different type of structure could also be identified in the tracheal wall. This fibre was much more branching in nature with termination sites as far apart as 6 mm (Fig. 6*D*). The fibre in Fig. 6*D* was purposely selected from the preparation (AAV2/2), in which only a limited number of structures was detected, in order to demonstrate the feasibility of the study of a single branching fibre. Based on extensive physiological studies that show that the principal vagal sensory nerve type other than capsaicin-insensitive Aδ-'cough' receptors in the guinea pig trachea are capsaicin-sensitive fibres, it is likely that this structure corresponds to a capsaicin-sensitive nociceptor (Riccio *et al.* 1996; Canning *et al.* 2004; Undem *et al.* 2004). In the living tissue the green fluorescent signal in the putative C-fibre structures was often weaker than in most Aδ-fibres, but could be amplified in fixed whole-mount preparations by using anti-GFP antibody (Fig. 6*E* and *F*). Figure 6*F* shows a terminal structure of a single vagal fibre in the whole-mount preparation of oesophageal mucosa/submucosa in which the fluorescent signal was amplified by staining with anti-GFP antibody. These results demonstrate feasibility of immunohistochemical staining for detailed histological analysis of terminal structures.

That the eGFP is also transported centrally was shown by the bright fluorescence of terminals in the nucleus of solitary tract (nTS) of the brainstem 1 month after bilateral injections of the AAV2/8 into the nodose ganglia ($n = 4$, Fig. 7). In addition to afferent nerve fibres the vagus nerves contain efferent fibres originating in the brainstem vagal motor nuclei (e.g. dorsal motor nucleus and nucleus ambiguus). Importantly, we did not observe green fluorescence-containing cell bodies in the vagal motor nuclei or any other area of the examined brainstem

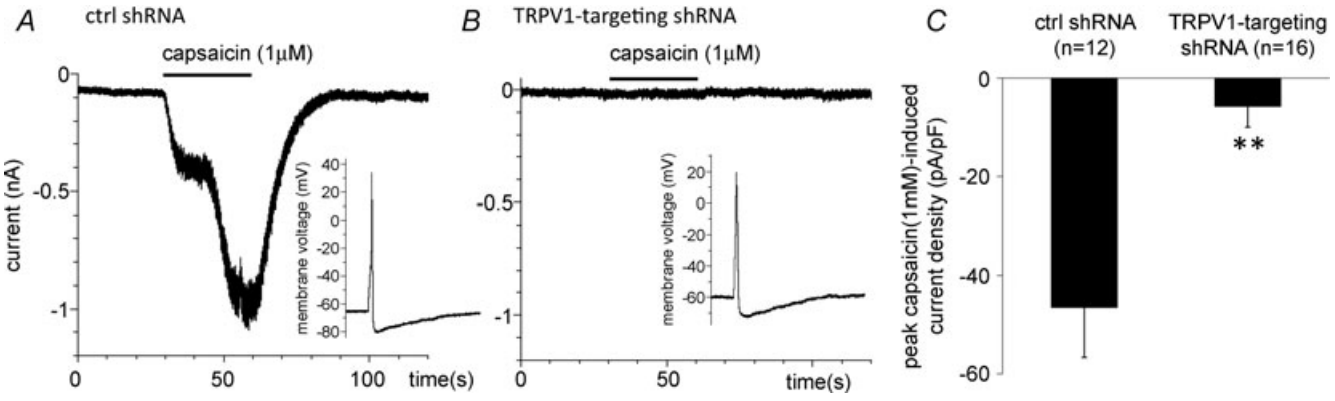

Figure 5. Knock-down of TRPV1 function in vagal jugular neurons after *in vivo* transduction with AAV2/8 encoding TRPV1-targeting shRNA

Whole cell gramicidin perforated patch clamp study in eGFP-positive jugular 5–6 weeks following the injection of AAV2/8 encoding shRNAs. *A*, example of the capsaicin-evoked inward current (voltage clamp) in control shRNA-transfected jugular neurons (similar robust current was evoked in 10 of 12 studied neurons). *B*, capsaicin failed to stimulate the majority (11/16) of TRPV1-targeting shRNA-transfected neurons. Insets in *A* and *B*, current injection (1 nA, 2 ms) evoked an action potential in all studied neurons (current clamp mode). *C*, mean data. $^{**}P < 0.01$, unpaired *t* test.

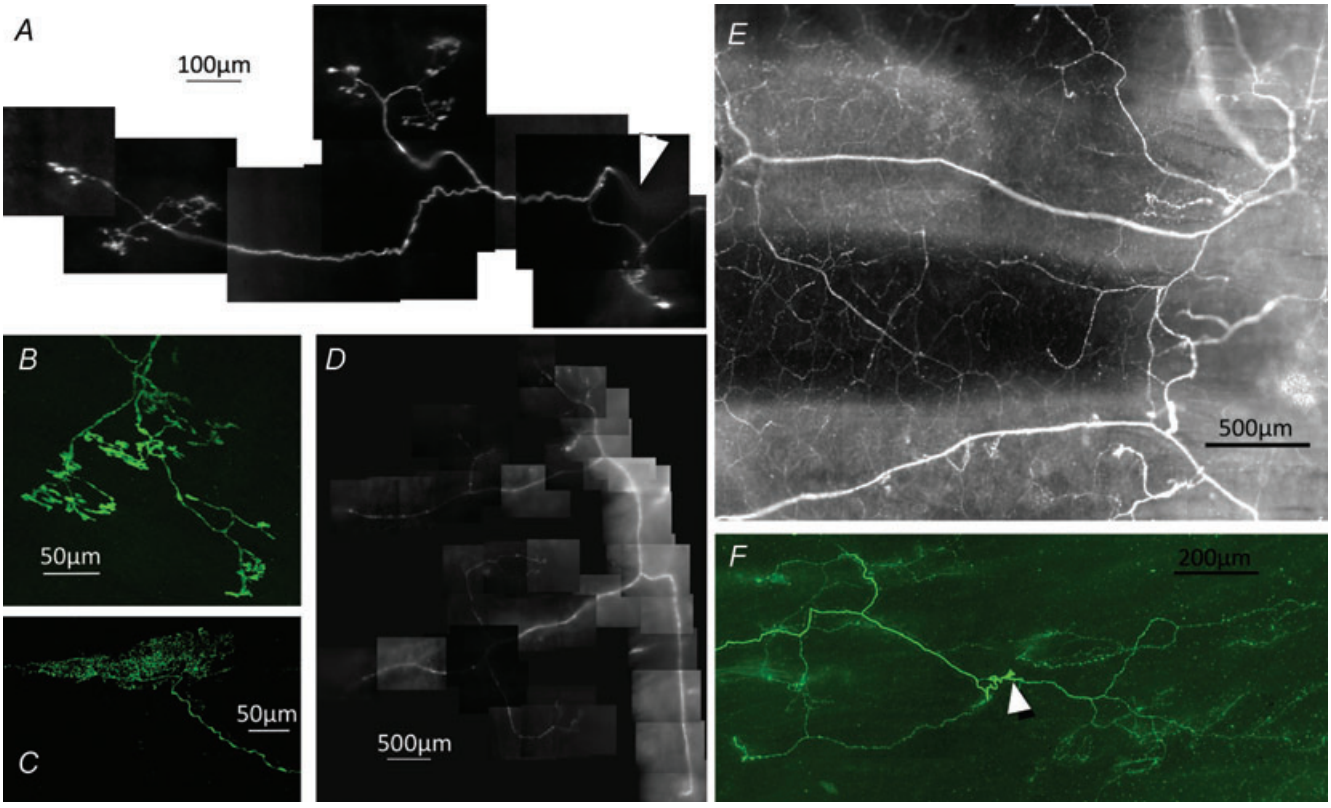

Figure 6. Visualization of peripheral vagal afferent nerve terminals
A, branching nodose Aδ-fibre in the trachea visualized in fresh tracheal tissue (tracheal epithelium was removed by gentle swab). Arrowhead indicates the parent fibre. *B*, confocal images of the nodose Aδ-fibre terminal structure in the trachea, and *C*, single intraganglionic laminar ending visualized in a sample containing the muscle and myenteric layers of the oesophagus. *D*, putative structure of a vagal C-fibre in the trachea (fixed whole-mount preparation). *E* and *F*, amplification of fluorescent signal with antibody against GFP; *E*, vagal afferent nerve terminal structures in the whole-mount preparation of trachea and *F*, oesophagus (oesophageal mucosa/submucosa, arrowhead indicates the parent fibre). Preparations in *A*–*D* were prepared from tissues harvested 4–6 weeks after unilateral injection of AAV2/2 (10^{12} PFU ml^{-1}) into right nodose ganglia. Preparations in *E*–*F* were prepared from tissues harvested 4–5 weeks after bilateral nodose injection of AAV2/8 (10^{13} PFU ml^{-1}). No signal was detected with antibody against GFP in control tissues from naïve animals.

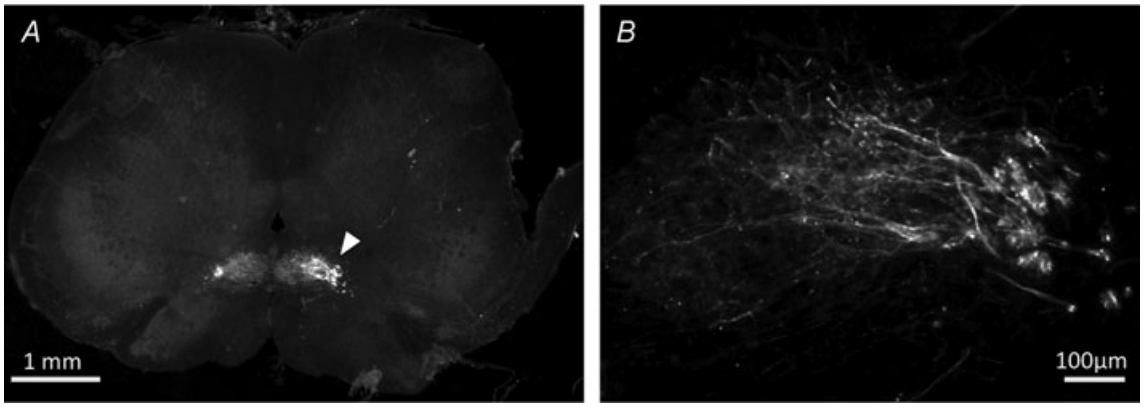

Figure 7. Visualization of central vagal afferent nerve terminals
Nerve fibres in solitary tract and their terminations in nucleus of solitary tract in transversal brainstem section after bilateral nodose injection of AAV2/8 (10^{13} PFU ml^{-1}). Arrowhead in *A* indicates the area magnified in *B*.

(Fig. 7; $n = 4$ animals, see Methods). Consistent with this observation, no fluorescent oesophageal motor endplates were noted in the oesophageal striated muscle although vagal afferent terminals (intraganglionic laminar endings that are located between the longitudinal and circular muscle) were brightly fluorescent ($n = 5$ oesophagus preparations from 5 animals, not shown). These data support the hypothesis that the AAV selectively transduced the vagal sensory neurons, without transducing autonomic efferent nerves.

Discussion

The results present five new findings relevant to those interested in the structure and physiology of vagal sensory neurons. First, direct microinjection of various serotypes of AAV vectors (2/2, 2/7, 2/8, 2/9) into the nodose ganglion leads to effective and long-lasting transduction of the primary sensory neurons therein, with no apparent untoward effect on the health of the animal. When relatively large viral titres are used, nearly every neuron within the ganglion can be transduced. Second, direct injection of AAV vectors is selectively taken up by the sensory neurons, and not appreciably taken up by the parasympathetic preganglionic vagal axons. Third, the transduction of vagal neurons by AAV vectors *in vivo* is sufficiently efficient such that it can be used to functionally silence target genes (e.g. TRPV1) using shRNA techniques. Fourth, the eGFP produced by AAV vectors in vagal neurons is transported to both the central and peripheral terminals allowing for bright imaging of the nerve endings in living tissues in the absence of parasympathetic nerve contamination. This allows for structure–electrophysiological function studies of vagal afferent nerve endings. Fifth, the AAV vector is taken up by the vagal nerve terminals in visceral tissues (e.g. oesophageal wall) and transported back to the cell body, which may allow for tissue-specific gene silencing, as well as for location studies of central terminals of vagal sensory neurons in a tissue-specific manner.

Depending on the AAV vector titre, as many as nearly 90% of the vagal sensory ganglion neurons could be transduced with the vector, as indicated by the expression of eGFP. This transduction is probably stable for long periods. We evaluated neurons 5 months after injection and still found that approximately 70% of nodose neurons were expressing eGFP. AAV vectors have been used to transduce neurons in DRG *in vivo*. Injection of the AAV into the spinal cord, DRG or into the sciatic nerve leads to transduction of spinal afferent neurons (Glatzel *et al.* 2000; Xu *et al.* 2003*a*; Storek *et al.* 2008; Towne *et al.* 2009; Mason *et al.* 2010). Depending on the route of delivery, certain AAV serotypes appear to be selective for small-diameter neurons with various efficacy of the transduction of large NF-positive neurons (Towne *et al.* 2009). In our study in which the vagal ganglion is directly injected, we observed no obvious selectivity in the transduction between small-diameter NF-negative and large-diameter-NF-positive neurons.

To determine if the virus transduction was efficient enough to introduce sufficient shRNA for effective gene silencing in vagal afferent neurons we chose shRNA targeting TRPV1. This is a convenient ion channel to evaluate as its function is easily quantified in vagal neurons using calcium assays or electrophysiology. Both the intracellular calcium increase responses and inward current response of vagal sensory neurons to capsaicin were reduced by nearly 90% in neurons from the ganglion treated with AAV vector constructed to produce TRPV1-targeting shRNA, whereas the capsaicin responses in neurons from ganglia treated with AAV producing a negative control RNA were not affected. These results prove that the AAV transduction of vagal ganglion neurons *in vivo* is a method that allows for long-lasting silencing of specific ion channels in the vagal sensory nerves. This should prove very useful in studies of the physiological role of ion channels where there are no selective antagonists available.

Even where there are antagonists available, the *in vivo* gene silencing with AAV vectors shown here has substantive advantages. Visceral tissues in general receive primary afferent innervation from vagal and spinal (DRG) neurons, and many tissues receive innervation from both nodose and jugular vagal neurons (Kummer *et al.* 1992; Wank & Neuhuber, 2001; Undem *et al.* 2004; Yu *et al.* 2005; Ni & Lee, 2008). Silencing TRPV1 gene expression *in vivo* with AAV injections would, for example, allow for evaluations of the relative role of vagal *vs.* spinal (DRG) sensory neurons in a physiological effect of *in vivo* capsaicin treatment or in the relative contributions of nodose *vs.* jugular vagal sensory neurons in a physiological response to capsaicin. This cannot be dissected using traditional chemical antagonists or currently available genetic knock-out strategies. With respect to using AAV vector-delivered shRNA silencing techniques to differentiate nodose *vs.* jugular neuronal responses, it was interesting to note that by contrast to the other serotypes, AAV2/2 remained delimited to the ganglion injected (Fig. 1*E*). When AAV2/8 serotype was injected into the nodose ganglion, we noted that 30–50% of the neurons within the juxtaposed jugular ganglion were transduced. The mechanism for this was not evaluated, but presumably involved either diffusion of the viral particles or uptake into the jugular axons traversing through the nodose ganglion and transport to the cell bodies.

Viruses are often taken up by sensory nerve terminals and transported to the cell soma. It was perhaps not surprising therefore, that we found AAV vectors were taken up by nodose nerve terminals innervating the oesophageal wall, and transported back to the cell body in the vagal sensory ganglia. The number of neurons transduced in this manner was quantitatively similar to the number of neurons retrogradely labelled by conventional tracer dye such as DiI. This provides a mechanism by which the expression of certain ion channel or receptor genes in vagal afferent neurons can be manipulated in a tissue-specific manner, without affecting the sensory neurons innervating other tissues. Our findings are consistent with the recent observations of Towne *et al.* (2009) who found that AAV injection into the glabrous plantar skin of the hindpaw, or into the triceps muscle, transduces DRG neurons innervating these tissues (Towne *et al.* 2009).

That the GFP was transported to the peripheral terminals should prove useful in the characterization of the peripheral terminals within visceral tissue of vagal afferent neurons. We revealed how readily a single axon can be followed to its termination points in living tissues (e.g trachea and oesophagus). Inasmuch as the AAV2/8 vector did not transduce parasympthatetic axons, parasympathetic ganglion neurons or enteric neurons, the bright fluorescent images provide a strong primary afferent 'signal-to-background noise' ratio. This provides for an ideal method for morphological structure–function studies of visceral afferent neurons. The Aδ 'cough' fibres we evaluated had morphological features identical to those described previously using staining techniques in fixed tissues (Mazzone & McGovern, 2008; Mazzone *et al.* 2009). They did not end in a single termination point, but rather terminated in on average three to four branched sites (Fig. 6*A*). Each of the termination sites covered an area more than 200 μm across, much larger than the more refined termination of afferent fibres in the airway neuroepithelial bodies, for example. The branching and termination of the nodose Aδ-fibres was much more limited than that observed of a presumed C-fibre in the trachea (Fig. 6*D*).

The GFP produced by the virus was also transported to central terminals in the nucleus of solitary tract (nTS). This, combined with the fact that the vagal afferent neurons could be transduced to produce eGFP by injection of AAV vectors to the peripheral tissues, allows for the characterization of central projections of tissue-specific afferent nerves. Importantly, we observed no eGFP expression in any cell in the brainstem in any sites including the sites of presumed parasympathetic efferent innervation, revealing the selectivity of the method, and that very little virus transduces neurons via diffusion into preganglionic through fibres in the ganglion, or via systemic access.

References

Adriaensen D, Brouns I, Pintelon I, De Proost I & Timmermans JP (2006). Evidence for a role of neuroepithelial bodies as complex airway sensors: comparison with smooth muscle-associated airway receptors. *J Appl Physiol* **101**, 960–970.

Agostoni E, Chinnock JE, De Daly MB & Murray JG (1957). Functional and histological studies of the vagus nerve and its branches to the heart, lungs and abdominal viscera in the cat. *J Physiol* **135**, 182–205.

Asala SA & Bower AJ (1986). An electron microscope study of vagus nerve composition in the ferret. *Anat Embryol (Berl)* **175**, 247–253.

Canning BJ, Mazzone SB, Meeker SN, Mori N, Reynolds SM & Undem BJ (2004). Identification of the tracheal and laryngeal afferent neurones mediating cough in anaesthetized guinea-pigs. *J Physiol* **557**, 543–558.

Castro M, Griffiths D, Patel A, Pattrick N, Kitson C & Ladlow M (2004). Effect of chain length on transfection properties of spermine-based gemini surfactants. *Org Biomol Chem* **2**, 2814–2820.

Cummins TR, Rush AM, Estacion M, Dib-Hajj SD & Waxman SG (2009). Voltage-clamp and current-clamp recordings from mammalian DRG neurons. *Nat Protoc* **4**, 1103–1112.

Ehlert EM, Eggers R, Niclou SP & Verhaagen J (2010). Cellular toxicity following application of adeno-associated viral vector-mediated RNA interference in the nervous system. *BMC Neurosci* **11**, 20.

Evans CH, Cooney AM & DiPaolo JA (1975). Colony inhibition mediated by nonimmune leukocytes *in vitro* and skin reactivity *in vivo* as indices of tumorigenicity of guinea pig cultures transformed by chemical carcinogens. *Cancer Res* **35**, 1045–1052.

Gabella G & Pease HL (1973). Number of axons in the abdominal vagus of the rat. *Brain Res* **58**, 465–469.

Gao GP, Alvira MR, Wang L, Calcedo R, Johnston J & Wilson JM (2002). Novel adeno-associated viruses from rhesus monkeys as vectors for human gene therapy. *Proc Natl Acad Sci U S A* **99**, 11854–11859.

Glatzel M, Flechsig E, Navarro B, Klein MA, Paterna JC, Bueler H & Aguzzi A (2000). Adenoviral and adeno-associated viral transfer of genes to the peripheral nervous system. *Proc Natl Acad Sci U S A* **97**, 442–447.

Kollarik M, Ru F & Brozmanova M (2010). Vagal afferent nerves with the properties of nociceptors. *Auton Neurosci* **153**, 12–20.

Kummer W, Fischer A, Kurkowski R & Heym C (1992). The sensory and sympathetic innervation of guinea-pig lung and trachea as studied by retrograde neuronal tracing and double-labelling immunohistochemistry. *Neuroscience* **49**, 715–737.

Kwong K, Kollarik M, Nassenstein C, Ru F & Undem BJ (2008). P2×2 receptors differentiate placodal *vs.* neural crest C-fiber phenotypes innervating guinea pig lungs and esophagus. *Am J Physiol Lung Cell Mol Physiol* **295**, L858–L865.

Lee MG, Macglashan DW Jr & Undem BJ (2005). Role of chloride channels in bradykinin-induced guinea pig airway vagal C-fibre activation. *J Physiol* **566**, 205–212.

MacGlashan D Jr (1989). Single-cell analysis of Ca^{2+} changes in human lung mast cells: graded *vs.* all-or-nothing elevations after IgE-mediated stimulation. *J Cell Biol* **109**, 123–134.

Mason MR, Ehlert EM, Eggers R, Pool CW, Hermening S, Huseinovic A, Timmermans E, Blits B & Verhaagen J (2010). Comparison of AAV serotypes for gene delivery to dorsal root ganglion neurons. *Mol Ther* **18**, 715–724.

Mazzone SB & McGovern AE (2008). Immunohistochemical characterization of nodose cough receptor neurons projecting to the trachea of guinea pigs. *Cough* **4**, 9.

Mazzone SB, Reynolds SM, Mori N, Kollarik M, Farmer DG, Myers AC & Canning BJ (2009). Selective expression of a sodium pump isozyme by cough receptors and evidence for its essential role in regulating cough. *J Neurosci* **29**, 13662–13671.

Ni D & Lee LY (2008). Effect of increasing temperature on TRPV1-mediated responses in isolated rat pulmonary sensory neurons. *Am J Physiol Lung Cell Mol Physiol* **294**, L563–L571.

Riccio MM, Kummer W, Biglari B, Myers AC & Undem BJ (1996). Interganglionic segregation of distinct vagal afferent fibre phenotypes in guinea-pig airways. *J Physiol* **496**, 521–530.

Sant'Ambrogio G & Widdicombe J (2001). Reflexes from airway rapidly adapting receptors. *Respir Physiol* **125**, 33–45.

Storek B, Reinhardt M, Wang C, Janssen WG, Harder NM, Banck MS, Morrison JH & Beutler AS (2008). Sensory neuron targeting by self-complementary AAV8 via lumbar puncture for chronic pain. *Proc Natl Acad Sci U S A* **105**, 1055–1060.

Taylor-Clark TE, Kollarik M, MacGlashan DW Jr & Undem BJ (2005). Nasal sensory nerve populations responding to histamine and capsaicin. *J Allergy Clin Immunol* **116**, 1282–1288.

Towne C, Pertin M, Beggah AT, Aebischer P & Decosterd I (2009). Recombinant adeno-associated virus serotype 6 (rAAV2/6)-mediated gene transfer to nociceptive neurons through different routes of delivery. *Mol Pain* **5**, 52.

Undem BJ, Chuaychoo B, Lee MG, Weinreich D, Myers AC & Kollarik M (2004). Subtypes of vagal afferent C-fibres in guinea-pig lungs. *J Physiol* **556**, 905–917.

Wank M & Neuhuber WL (2001). Local differences in vagal afferent innervation of the rat esophagus are reflected by neurochemical differences at the level of the sensory ganglia and by different brainstem projections. *J Comp Neurol* **435**, 41–59.

Xu Y, Gu Y, Wu P, Li GW & Huang LY (2003*a*). Efficiencies of transgene expression in nociceptive neurons through different routes of delivery of adeno-associated viral vectors. *Hum Gene Ther* **14**, 897–906.

Xu Y, Gu Y, Xu GY, Wu P, Li GW & Huang LY (2003*b*). Adeno-associated viral transfer of opioid receptor gene to primary sensory neurons: a strategy to increase opioid antinociception. *Proc Natl Acad Sci U S A* **100**, 6204–6209.

Yu S, Ru F, Ouyang A & Kollarik M (2008). 5-Hydroxytryptamine selectively activates the vagal nodose C-fibre subtype in the guinea-pig oesophagus. *Neurogastroenterol Motil* **20**, 1042–1050.

Yu S, Undem BJ & Kollarik M (2005). Vagal afferent nerves with nociceptive properties in guinea-pig oesophagus. *J Physiol* **563**, 831–842.

Zagorodnyuk VP & Brookes SJ (2000). Transduction sites of vagal mechanoreceptors in the guinea pig esophagus. *J Neurosci* **20**, 6249–6255.

Zagorodnyuk VP, Chen BN, Costa M & Brookes SJ (2003). Mechanotransduction by intraganglionic laminar endings of vagal tension receptors in the guinea-pig oesophagus. *J Physiol* **553**, 575–587.

Author contributions

All authors contributed to conception and design of the experiments, collection, analysis and interpretation of data, drafting the article or revising it critically for important intellectual content. All authors approved the final version of the manuscript.

Acknowledgements

Supported by NIH DK074480 (M.K.) and HL062296 (B.J.U.). M.K. is also supported by Scientific Grant Agency, Slovak Republic (VEGA) grant 1/0276/10 and Center of Excellence for Research in Personalized Therapy (CEVYPET), EU grant.

Author's present address

C. J. A. Ring: Department of Natural Sciences, School of Health & Social Sciences, Middlesex University, London, UK.